Land-Use Practices and Biomass Burning: Impact on the Chemical Composition of the Atmosphere

Claire Granier, Wei Min Hao, Guy Brasseur, and
Jean-François Müller

Biomass burning results in the release of important amounts of gases and aerosols into the atmosphere. It has therefore a significant impact on the distribution of chemical species in the atmosphere (Crutzen et al. 1979; Andreae 1993; Hao and Ward 1993; Levine 1994). Biomass burning occurs mainly in the tropics, in relation to deforestation, shifting cultivation, fuel-wood use, and clearance of agricultural residues (Hao and Liu 1994). The tropical deforestation rate is believed to have increased by 40% during the last decade (Hao et al. 1994). The use of wood to produce energy is currently increasing at a rate of 3% per year. Burning of savanna to produce forage and burning agricultural may also have increased recently.

This chapter evaluates the contribution of biomass burning to the emissions of several trace gases, including carbon monoxide (CO), methane (CH_4), nitrogen oxides (NO_x), and some nonmethane hydrocarbons (NMHCs). The impact of such emissions on the atmospheric distribution of these gases, as well as their impacts on the formation of reactive trace species, such as ozone (O_3) and the hydroxyl radical (OH), are assessed. The effect of sulfur compounds and aerosols emitted by biomass burning is not considered here.

The Three-Dimensional Model

The model used in this study is a three-dimensional chemical/transport model of the troposphere named IMAGES (Intermediate Model for the Annual and Global Evolution of Species). A detailed description of the model is given by Müller and Brasseur (1995). The horizontal resolution of the model is 5° in latitude and in longitude. The model includes 25 layers from the ground to 50 mbar, which are expressed in sigma-coordinates. Monthly average distributions of winds, surface pressure, temperature, water vapor, and clouds are specified, according to climatological analyses from ECMWF (European Center for Medium Weather Range Forecast) and from ISCCP (International Satellite Cloud Climatology Project). The transport of long-lived species is formulated through advection, diffusion, and convection. Advective transport is represented by a semilagrangian scheme (Smolarkiewicz and Rasch 1991).

The model simulates the evolution of 40 species, among which 20 are transported: these species include reactive compounds of oxygen, hydrogen, and nitrogen, as well as 6 nonmethane hydrocarbons (ethylene, ethane, propylene, isoprene, α-pinene, and a lumped species used as a surrogate for all other hydrocarbons). Approximately 120 chemical and 20 photodissociation reactions are considered. The emissions for chemical species by natural or anthropogenic sources have been compiled by Müller (1992), at a spatial resolution of 5° in latitude by 5° in longitude.

Distribution of Emission of Gases from Biomass Burning

The spatial and temporal distributions of the amount of biomass burned in tropical regions are taken from the data base established by Hao and Liu (1994). This data base provides the data for the amount of biomass burned monthly, at a 5°-by-5° resolution, for the reference year 1980. It accounts for the fires resulting from deforestation, shifting cultivation, savanna burning, fuel-wood use, and burning of agricultural residues. In nontropical areas, the amount of biomass burned is determined by Müller (1992), using statistics established by OECD (1989), USDA Forest Service (1986), and the United Nations (1988).

The amount of CO_2 emitted from biomass burning is first estimated assuming that the carbon content of biomass is about 50%, and that the fuel carbon is released as CO_2, CO, CH_4 and nonmethane hydrocarbons. The emission of each chemical species relative to CO_2 is then computed for each type of biomass fire (Hao and Ward 1993; Hao unpublished results). The emission ratios of CH_4, CO, or several nonmethane hydrocarbons (NMHCs) to CO_2 are given in table 14.1. It should be noted that in table 14.1, as well as in the rest of this chapter, "other" NMHCs do not

Table 14.1 Emission ratios to CO_2 from biomass burning (in percentages by volume)

	CO	CH_4	NO_x	C_2H_4	C_2H_6	C_3H_6	Other NMHCs
Tropical forest	12.4[a]	1.57[a]	0.21[b]	0.36[b]	0.116[b]	0.107[b]	0.16[b]
Temperate/boreal forest	14.94	1.05	0.21	0.24	0.078	$7.4\ 10^{-2}$	0.107
Savanna	4.17	0.24	0.074	0.05	$1.78\ 10^{-2}$	$1.63\ 10^{-2}$	$2.4\ 10^{-2}$
Fuel wood	9.89	2.49	0.065	0.57	0.184	0.169	0.25
Agriculture waste	8.70	0.44	0.19	0.1	$3.26\ 10^{-2}$	$2.99\ 10^{-2}$	$4.5\ 10^{-2}$

a. Data for CO and CH_4, revised from Hao and Ward (1993).
b. Data for other species from Hao et al. (1995) and Hao (Unpublished results).

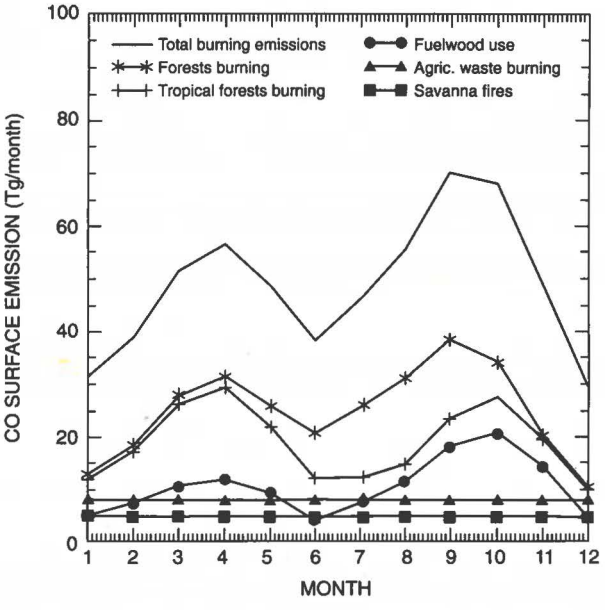

Figure 14.1 Seasonal variation of the CO emissions from tropical and total forests burning, savanna fires, fuel-wood, and agricultural waste burning, and from all sources of biomass burning, in Tg CO per month

include isoprene or terpenes, because the emission of these species from fires is insignificant.

Emissions of the trace gases vary significantly with season, following the seasonal variation of the total amount of biomass burned as shown by Hao and Liu (1994). Figure 14.1 shows the seasonal variation of the global amount of CO emitted by biomass burning and from each of the four types of biomass fires considered here. It should be noted that, although savanna burning represents the largest source of CO_2, its relative importance for the emissions of CO and of other trace gases is very low, due to the low emission ratios typical for this type of fire. Forest burning, more particularly tropical forests burning as shown in figure 14.1, accounts for about half of the trace gas emissions of CO and other trace gases from biomass burning.

Table 14.2 presents the annual emissions of CO, CH_4, and NMHCs from various sources. It shows, for example, that biomass burning represents the largest source of CO (586 Tg/year, accounting for approximately 45% of the total surface source of CO). Biomass burning contributes significantly to the emissions of the NMHCs (45% in the case of ethylene). The contributions of biomass burning to the sources of CH_4 and NO_x are smaller, and represent only 8 and 13% of the source, respectively. The emissions of NO_x associated with biomass burning are, however, important because they take place mostly in nonindustrialized areas of the tropics.

The global emission estimates from biomass burning given in table 14.2 are lower than those presented in Müller (1992), since the emission factors used by Müller (1992) were generally higher and not dependent on the type of ecosystem. When compared to other estimates (Andreae 1993; Bonsang et al. 1994; Levine et al. 1994), the emission factors relative to CO_2 given here are significantly lower for savanna burning and slightly higher for forest fires than those used in previous studies, resulting in lower emissions of trace gases from biomass burning. However, the total emissions from biomass burning presented here are well within the range given by WMO/UNEP (1995) (i.e., 400–700 Tg/yr for CO, 20–80 Tg/yr for CH_4, 3–13 Tg N/yr for NO_x), but are lower than the WMO/UNEP estimate of 30–90 Tg C/yr for NMHCs.

Results of the Simulations

Several model simulations were performed to assess the importance of biomass burning on the global budget of several tropospheric species. Two cases were compared: the reference case, in which all sources of

Table 14.2 Annual emissions of trace gases

	CO (Tg CO/y)	CH_4 (Tg CH_4/y)	NO_x (Tg N/y)	C_2H_4 (Tg C/y)	C_2H_6 (Tg C/y)	C_3H_6 (Tg C/y)	Other NMHCs (Tg C/y)
Forest burning	299	19	2.4	3.4	1.1	1	1.5
Tropics	233	17	2	2.9	0.9	0.9	1.3
Mid and high latitude	66	3	0.4	0.5	0.1	0.1	0.2
Savanna burning	128	4	1.1	0.7	0.2	0.2	0.3
Fuel-wood use	98	14	0.3	2.4	0.8	0.7	1.1
Agricultural waste	61	2	0.7	0.3	0.1	0.1	0.1
Total biomass burning	586	39	4.5	6.8	2.2	2.0	3.0
Anthropogenic emissions	383	131	23.4	2.1	3	0.6	16.9
Ocean + soils + other sources	330	300	6.6	6.2	0.8	3.7	35.1
Total emissions	1299	470	34.5	15.1	6.0	6.3	55

tropospheric species are included, and a simulation in which the biomass burning source is excluded. In order to better quantify the contribution of each burning source to the budget of the tropospheric chemical species, four additional simulations were performed, in which only one source was considered at a time.

Carbon Monoxide and Nonmethane Hydrocarbons

Since biomass burning represents almost half of the total CO source, as shown in table 14.2, such a source should have a large impact on the atmospheric CO distribution. Figure 14.2*a* shows the surface CO distribution in October, when all sources are included. The CO concentration reaches maxima in the industrialized regions and in the tropics. Figure 14.2*b* shows the change in the CO mixing ratio at the surface level (October) resulting from biomass burning emissions. The CO concentration increases at all latitudes. This increase is greater than 20% everywhere and reaches maximum values of 300% over the areas where biomass burning takes place. The corresponding change in the zonally averaged CO mixing ratio as a function of latitude and height is displayed in figure 14.2*c*. The largest changes in October (about 80%) take place in the southern tropics during the dry season. Large amounts of CO from biomass burning are efficiently transported to the upper troposphere by convection, and redistributed towards higher latitudes in the Southern Hemisphere. The CO increase is minimum in the 10–30°N latitude band, where other CO sources (i.e., biogenic and methane oxidation) dominate. The higher values calculated for the northern mid and high latitudes are due to temperate and boreal forest fires.

The global CO burden increases in October by about 45% as a result of biomass burning. A similar behavior is observed for all seasons, the increase in the tropospheric CO burden due to biomass burning varying from 30% in February to 45% in October, as a result of seasonal changes in the amount of biomass burned.

Simulations in which each biomass burning source is isolated show that, in South America, the increases in the CO mixing ratio associated with biomass burning result for about two thirds from forest fires, the remaining being mostly due to savanna fires. The CO increase in southern Africa is mostly due to savanna burning, which is most pronounced in this area during October, and the CO increase over equatorial Africa is mainly the result of forest burning. Forest fires and fuel-wood use are the main causes of the CO increase in southern Asia.

Table 14.3 provides the global budget of CO (annual mean) in the troposphere as calculated by the model, and the contribution of each source to the global burden of CO. These values show the importance of biomass burning for the determination of the CO tropospheric burden: about 26% of the tropospheric CO burden results from biomass burning. The tropospheric CO burden evaluated here is about 10% lower than in the previous estimate of Müller and Brasseur (1995) due to lower emissions from biomass burning, especially from the savanna fires.

Biomass burning represents 45%, 37%, 32%, and 5% of the total source of ethylene, ethane, propylene, and other NMHCs, respectively (see table 14.2). The global distribution of these compounds should there-

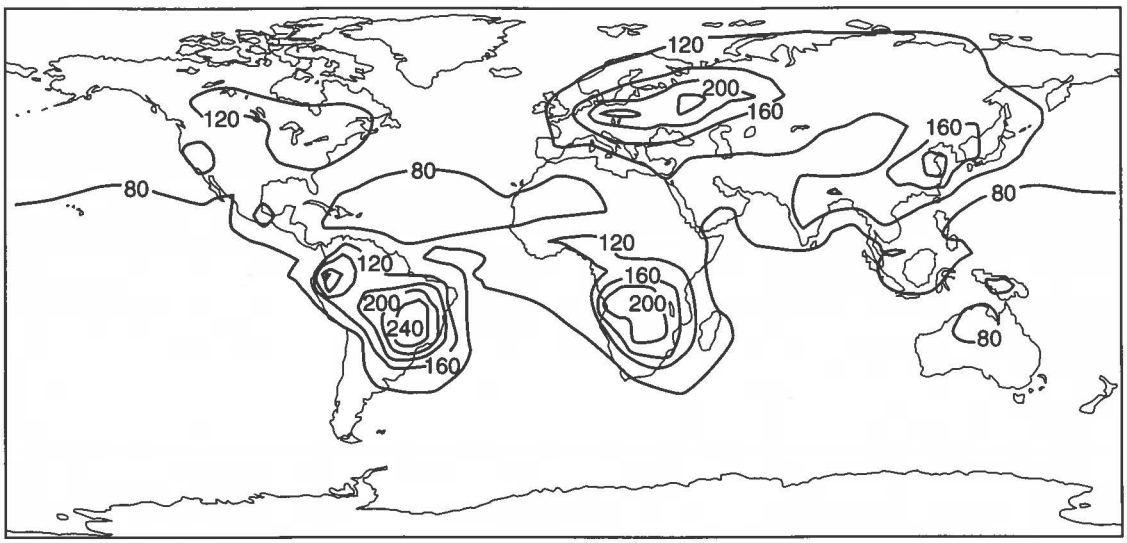

Contour Levels (ppbv) = (0, 40, 80, 120, 160, 200, 240, 280) (a)

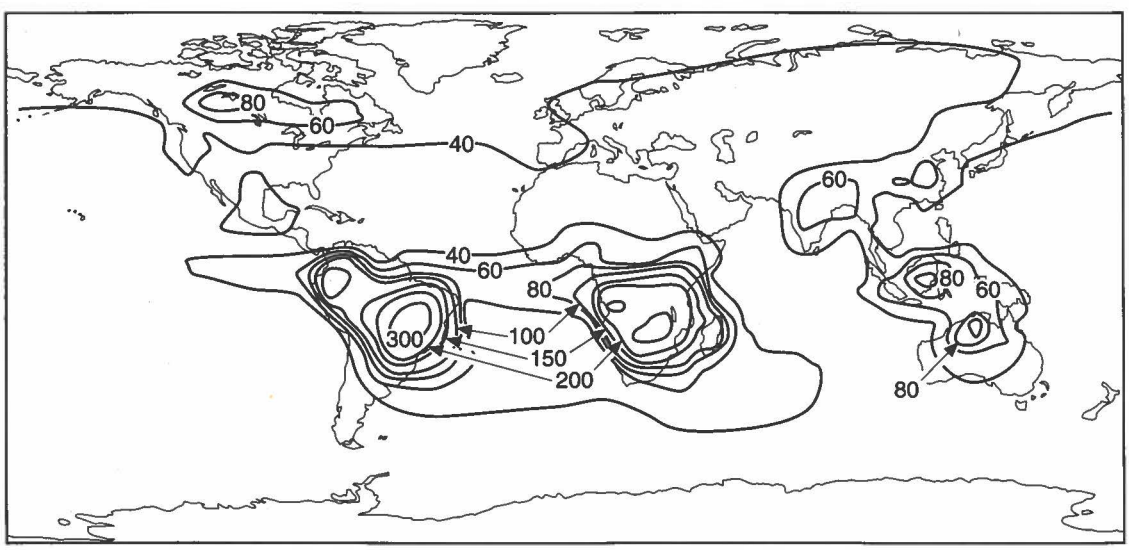

Contour Levels (%) = (0, 20, 40, 60, 80, 100, 150, 200, 300, 400) (b)

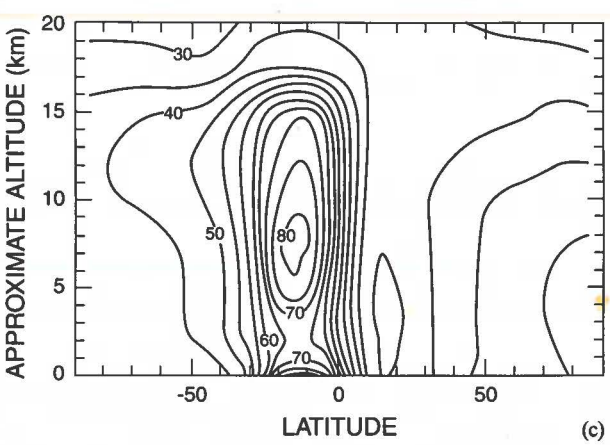

(c)

Figure 14.2 (*a*) CO mixing ratio distribution at the surface in October. (*b*) Change in the CO mixing ratio in October resulting from biomass burning emissions at the surface level and (*c*) as a function of latitude and altitude (zonal average)

Table 14.3 CO tropospheric budget (Tg CO/y)

Total emissions	1299 Tg/y
Emission from biomass burning	585 Tg/y
Photochemical production	946 Tg/y
Photochemical loss	2016 Tg/y
Dry deposition	229 Tg/y
CO burden—all sources	327 Tg
Forest burning	41 Tg
Savanna burning	15 Tg
Fuel-wood use	17 Tg
Agricultural waste	9 Tg
Total biomass burning	82 Tg

fore be largely affected by biomass burning. Figure 14.3 shows the change in the ethane (figure 14.3*a*) and ethylene (figure 14.3*b*) surface mixing ratios resulting from biomass burning in October. The mixing ratio of C_2H_6 increases by approximately a factor of 4 over biomass burning areas. As C_2H_6 has a relatively long lifetime (about 80 days), it can be transported to mid and high latitudes, like CO. This is not the case for C_2H_4, whose lifetime is on the order of 1 day. Hence, the additional ethylene concentration due to biomass burning remains near the source areas. Table 14.4 presents the percentage change in the tropospheric NMHCs burdens (annual mean) from a no-biomass burning case to a case in which each biomass burning source is considered separately. Forest fires and fuel-wood use have the greatest impact on the NMHCs surface mixing ratio.

Nitrogen Oxides

Biomass burning accounts for approximately 13% of the global NO_x (which represents the sum $[NO]+[NO_2]$) source (see table 14.2). Figure 14.4 represents the change in the NO_x concentration at the surface resulting from biomass burning. In contrast with CO, NO_x has a short lifetime, so that it is less efficiently transported. The observed increase in the NO_x mixing ratio is therefore located near the sources of biomass burning, where the NO_x increase can be very high. As for CO, increases in the NO_x concentration over South America and southern Africa are mostly due to forest and savanna burning, while changes over Asia result mainly from fuel-wood and agricultural waste burning. It should be noted that the concentration of other nitrogen compounds such as HNO_3, which have a longer lifetime than NO_x, or such as PAN, which is affected by the increased NMHCs and NO_x emissions can also increase significantly at mid and high latitudes, away from the source areas.

A yearly averaged global budget for NO_x is given in table 14.5. Because the impact of biomass burning on the NO_x distribution is quite localized and remains significant only in the lowest layers of the atmosphere, biomass burning contributed to only 14% of the tropospheric NO_x burden in the model.

Ozone and the Hydroxyl Radical

As a consequence of the increase in the concentrations of the ozone precursor (i.e., CO, NMHCs, and NO_x), the ozone production is expected to increase as a result of biomass burning. This increase should affect the whole troposphere, due to vertical transport by advection and convection of the ozone precursors. The model predicts a 19% increase in the globally averaged net photochemical production of ozone (annual mean) resulting from biomass burning. This value is slightly higher than the value suggested by Bonsang et al. (1994), who evaluated the net ozone production in the troposphere from biomass burning in the tropics as being about 10% of the total ozone production. Such an increase leads to an enhanced concentration of ozone at the surface, as shown in figure 14.5*a*. Figure 14.5*b* displays the corresponding change in the vertical ozone distribution. The ozone concentration increases at all latitudes and altitudes by at least 5%, with maximum values around 100% in the vicinity of biomass burning areas.

The impact of biomass burning on the hydroxyl radical concentration is more complex (figure 14.6*a* and *b*). The increase in CO at all altitudes explains the calculated decrease of OH in the free troposphere and at mid latitudes. Near the source regions, however, the higher ozone concentrations result in an enhanced OH production. At the same time, the higher conversion of HO_2 to OH associated with the increase in nitrogen oxide concentration produces an increase (up to 10^6 cm^{-3} or 100%) in the OH density above the source areas.

The OH concentration determines the lifetime of most tropospheric species. When biomass burning is included in the model simulations, the OH concentration can either increase or decrease in different areas, so that the change in the globally averaged OH concentration is small. Consequently, the impact of biomass burning on the global lifetime of long-lived species is limited. For example, the yearly global average lifetime of methane changes from 9.66 years when biomass burning is ignored to 9.86 years when biomass

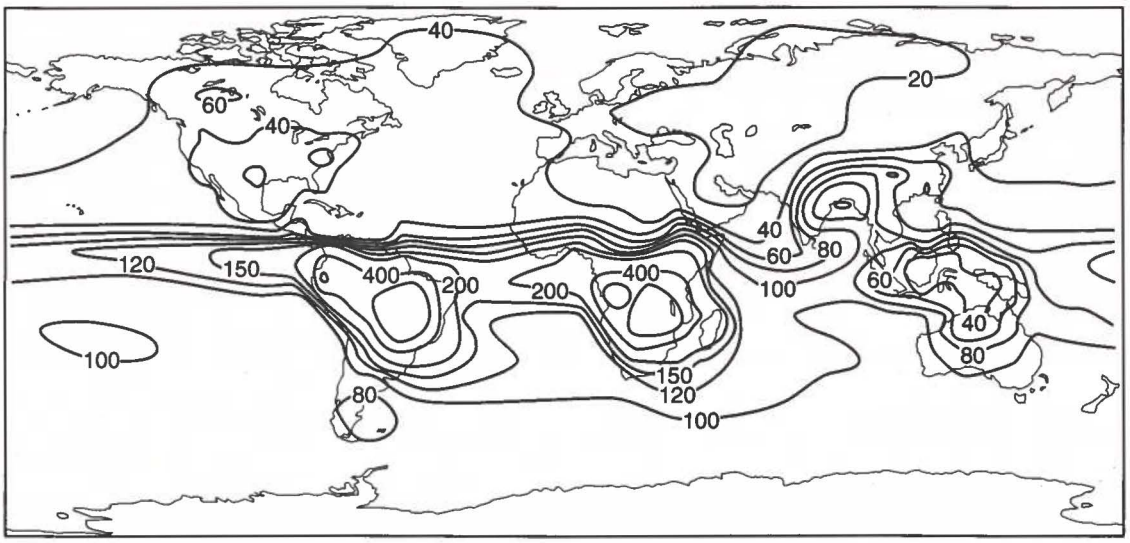

Contour Levels (%) = (0, 20, 40, 60, 80, 100, 120, 150, 200, 400, 600) (a)

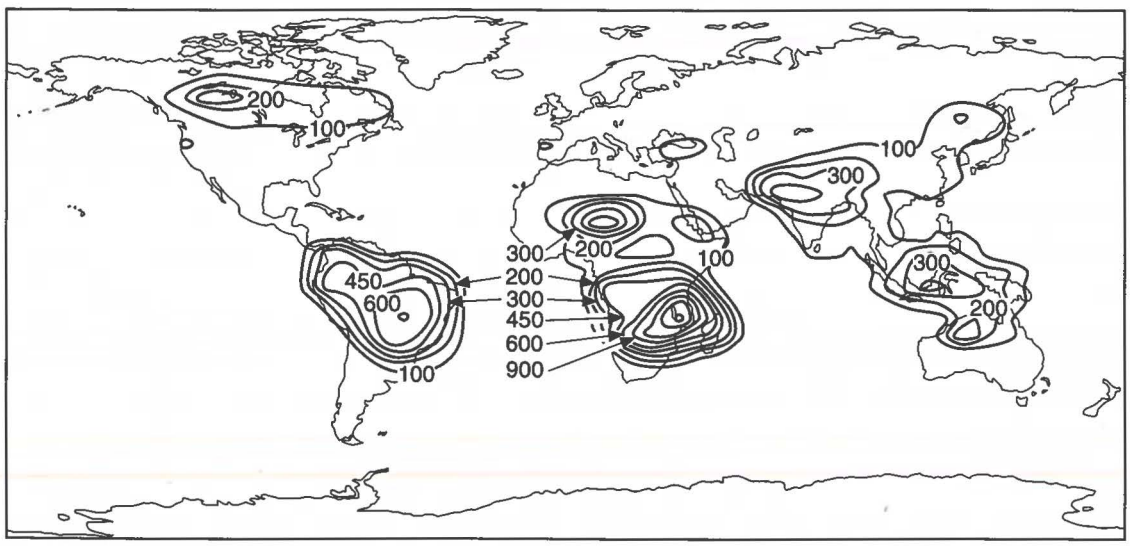

Contour Levels (%) = (0, 100, 200, 300, 450, 600, 900, 1200, 1500, 1800) (b)

Figure 14.3 Change in the (*a*) ethane and (*b*) ethylene surface mixing ratios resulting from biomass burning in October

Table 14.4 Percentage increase in the NMHCs tropospheric burdens due to biomass burning averaged yearly

	C_2H_4	C_2H_6	C_3H_6	Other NMHCs
Forest burning	17%	23%	11%	2.8%
Savanna burning	3%	4.3%	1.5%	0.2%
Agriculture waste burning	3%	2.9%	1.4%	0.8%
Fuel-wood burning	21%	19%	12%	2.4%
Total	44%	49.2%	25.9%	6.2%

Table 14.5 NO_x tropospheric budget (Tg N/y)

Total emissions	34.5 Tg/y
Emission from biomass burning	4.5 Tg/y
Photochemical production	71.6 Tg/y
Photochemical loss	100 Tg/y
Dry deposition	4.5 Tg/y
NO_x burden	
All sources	0.52 Tg
Due to biomass burning	0.02 Tg

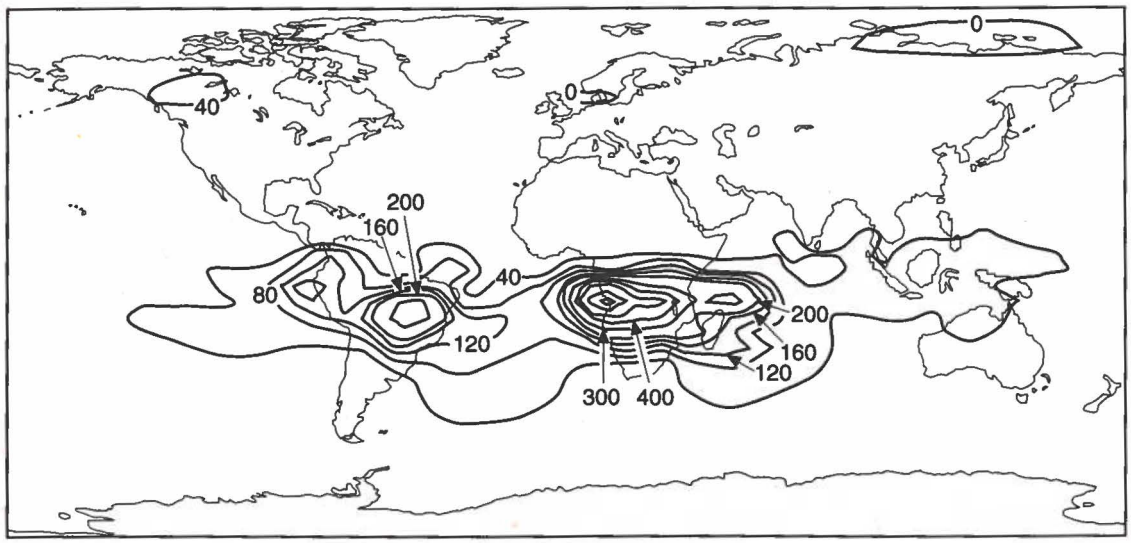

Contour Levels (%) = (0, 40, 80, 120, 160, 200, 300, 400, 500, 1000, 1500)

Figure 14.4 Change in the NO_x concentration at the surface resulting from biomass burning emissions in October

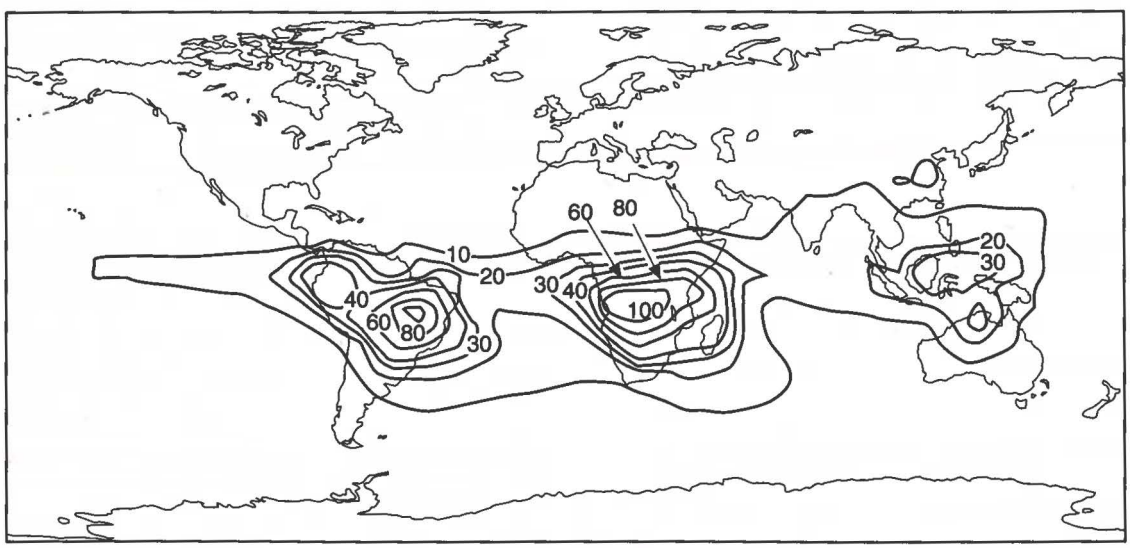

Contour Levels (%) = (0, 10, 20, 30, 40, 60, 80, 100, 120) (a)

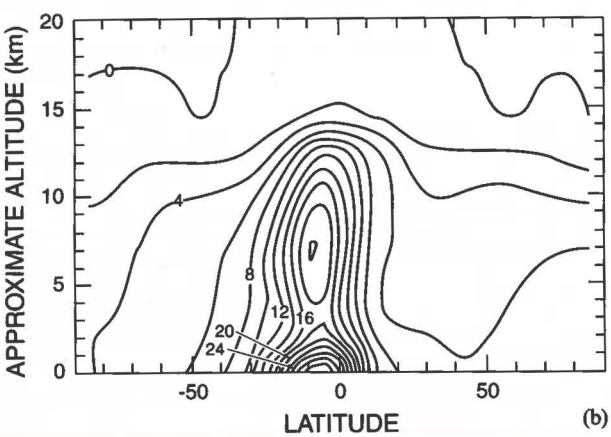

(b)

Figure 14.5 Change in the ozone mixing ratio in October resulting from biomass burning at (*a*) the surface level and (*b*) as a function of latitude and altitude (zonal average)

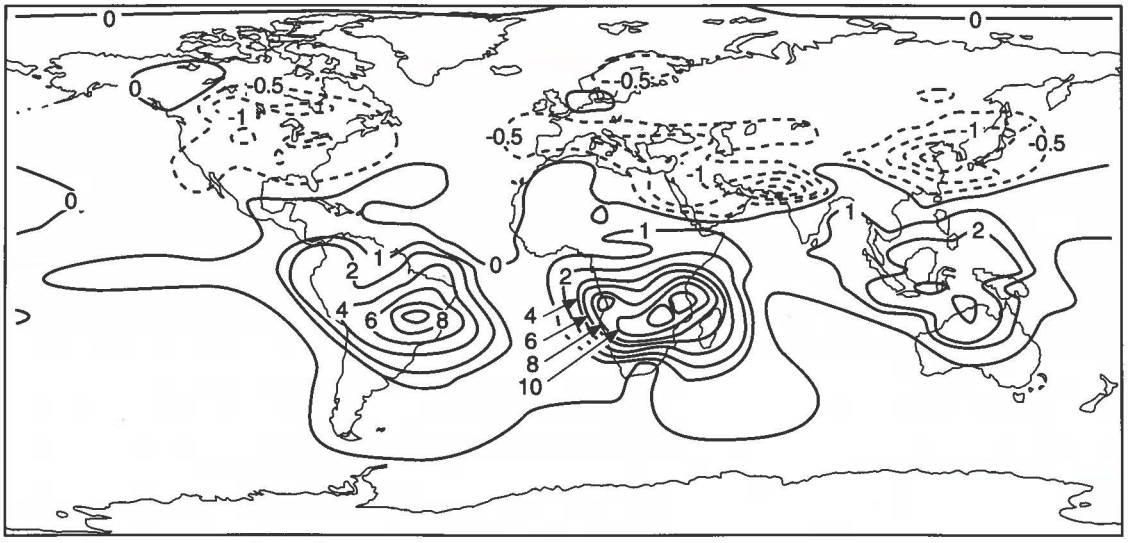

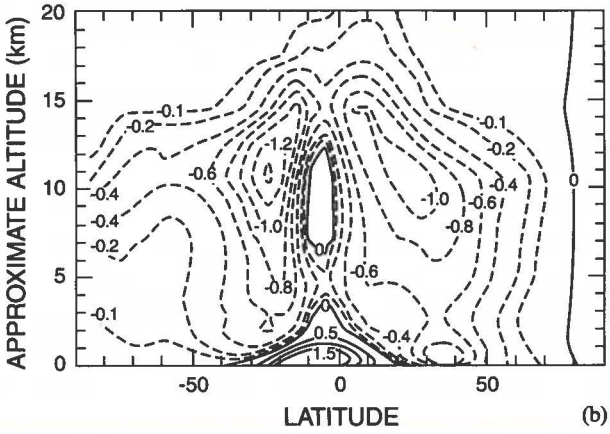

Figure 14.6 Change in the OH concentration in October resulting from biomass burning (*a*) at the surface level and (*b*) as a function of latitude and altitude (zonal average)

burning is included, which corresponds to a change of less than 2%.

Conclusions

This chapter confirms the large contribution of biomass burning to the emissions of CO, CH_4, NO_x, and nonmethane hydrocarbons: biomass burning represents about 45% of the surface source of CO and of ethylene, and 8 and 13% of the total source of CH_4 and NO_x, respectively. The impact of such sources on the chemical composition of the troposphere has been assessed with a three-dimensional model. It has been shown that trace gases emitted from biomass burning produce significant increase in the concentration of several tropospheric compound concentrations on the global scale. As a result of biomass burning, ozone concentrations increase by up to 100% in the tropical burning areas, and by at least 5% at higher latitudes. The concentration of the hydroxyl radical, which determines to a large extent the oxidizing capacity of the atmosphere, either increases or decreases depending on the area, but its globally averaged concentration change is rather small.

Acknowledgments

The National Center for Atmospheric Research is sponsored by the National Science Foundation. Claire Granier is supported by NASA, under contract No.

W-18,531. Jean-François Müller is research assistant of the Belgian Fonds de la Recherche Scientifique. This work was partly supported by the Belgian Federal Office for Scientific, Technical and Cultural Affairs (O.S.T.C.).

References

Andreae, M. O. 1993. The influence of tropical biomass burning on climate and the atmospheric environment, in *Biogeochemistry of Global Change*, Ed. R. S. Oremland, Chapman and Hall, New York, pp. 113–150.

Bonsang, B., M. Kanakidou, and C. Boissard. 1994. Contribution of tropical biomass burning to the global budget of hydrocarbons, carbon monoxide, and tropospheric ozone, in *Non-CO_2 Greenhouse Gases*, Eds. J. van Ham et al., Kluwer Academic Publishers, Dordrecht, the Netherlands.

Crutzen, P. J., L. E. Heidt, J. P. Krasnec, W. H. Pollock, and W. Seiler. 1979. Biomass burning as a source of atmospheric trace gases, *Nature*, 282, 253–256.

Hao, W. M., and D. E. Ward. 1993. Methane production from global biomass burning, *J. Geophys. Res.*, 20 657–20 661.

Hao, W. M., and M.-H. Liu. 1994. Spatial distribution of tropical biomass burning in 1980 with $5° \times 5°$ resolution, *Global Biogeochem. Cycles*, 8, 495–503.

Hao, W. M., M.-H. Liu, and D. E. Ward. 1994. Impact of deforestation on biomass burning in the tropics, in *Proceedings of Global Climate Change: Science, Policy, and Mitigation Strategies*, Ed. C. V. Mathai and G. Stensland, Air and Waste Management Association, 273–278.

Hao, W. M., D. E. Ward, G. Olbu, and S. P. Baker. 1995. Emissions of CO_2, CO, and hydrocarbons from fires in diverse African savanna ecosystems, *J. Geophys. Res.* special SAFARI issue, in press, 1996.

Levine, J., W. Cofer, and J. Pinto. 1994. Biomass burning, in *Atmospheric Methane: Source, Sinks, and Role in Global Change*, Ed. M. Khalil, NATO/ASI Series, Ch. 14, 299–313.

Müller, J. F., and G. Brasseur. 1995. IMAGES: A three-dimensional chemical transport model of the global troposphere, *J. Geophys. Res.*, June.

OECD. 1989. Organization for Economic Cooperation and Development/International Energy Agency, Quarterly oil statistics and energy balances, fourth quarter 1988, Paris.

Smolarkiewicz, P. K., and P. J. Rasch. 1991. Monotone advection on the sphere: An Eulerian versus semi-Lagrangian approach, *J. Atmos. Sci.*, 48, 793–810.

United Nations (UN). 1988. Statistiques de l'environnement en Europe et en Amérique du Nord, Recueil expérimental, *Normes et Etudes Statistiques*, vol. 39, New York.

USDA. 1986. United States Forest Service, An analysis of the timber situation of the United States, Appendix 3.

WMO/UNEP. 1995. *Scientific Assessment of Ozone Depletion: 1994.* World Meteorological Organization, Geneva, Switzerland.